Structured carbons as supports for hydrogenation hybrid catalysts prepared by the immobilization of a Rh diamine complex

Constanta Cristina Gheorghiu, Enrique García-Bordejé, Nathalie Job, M. Carmen Román-Martínez

PII: S1385-8947(16)30039-0
DOI: http://dx.doi.org/10.1016/j.cej.2016.01.071
Reference: CEJ 14690

To appear in: *Chemical Engineering Journal*

Received Date: 6 November 2015
Revised Date: 18 January 2016
Accepted Date: 22 January 2016

Please cite this article as: C.C. Gheorghiu, E. García-Bordejé, N. Job, M. Carmen Román-Martínez, Structured carbons as supports for hydrogenation hybrid catalysts prepared by the immobilization of a Rh diamine complex, *Chemical Engineering Journal* (2016), doi: http://dx.doi.org/10.1016/j.cej.2016.01.071

Structured carbons as supports for hydrogenation hybrid catalysts prepared by the immobilization of a Rh diamine complex

Constanta Cristina Gheorghiu[a], Enrique García-Bordejé[b], Nathalie Job[c], M.Carmen Román-Martínez[a*]

[a]Department of Inorganic Chemistry and Materials Institute, University of Alicante, Carretera de San Vicente s/n. E-03690 Alicante, Spain

[b]Instituto de Carboquímica (ICB-CSIC), Miguel Luesma Castán 4, E-50018 Zaragoza, Spain

[c]Department of Chemical Engineering – Nanomaterials, Catalysis, Electrochemistry, University of Liège (B6a), Sart-Tilman, B-4000 Liège, Belgium

* mcroman@ua.es

Abstract

A CNF-monolith sample (carbon nanofibres grown on a ceramic monolith), and a granular carbon xerogel have been used as supports for hybrid catalysts where the active species is an Rh diamine complex. The advantages of these supports are their open porous structure and their morphology, which make catalyst handling easier and avoid difficult separation processes. The obtained catalysts are noticeably more active than the homogeneous Rh complex and are stable against leaching. At first use, partial reduction of the Rh complex takes place and nanometer-sized Rh particles develop, which increases the catalyst activity. Despite the open porous structure, mass transport limitations are present, especially in the case of the carbon xerogel based catalyst. Differences in internal mass transfer limitations are essentially due to the different diffusional path lengths.

Keywords: carbon xerogel, CNF-monolith, structured supports, hybrid catalyst, hydrogenation

1. Introduction

Carbon materials are recognized as suitable supports in heterogeneous catalysis due to specific characteristics such as the broad variety of morphological, textural and chemical properties (adjustable up to certain limits), resistance to acidic/basic media, and the potential easy recovery of precious metals by support burn out [1,2]. Besides,

the following properties are usually required: (i) high purity, avoiding either catalyst poisoning or the promotion of unwanted side reactions, (ii) large volumes of meso/macropores to avoid diffusional limitations, and (iii) potential specific metal-support interactions that can yield positive effects on the catalytic activity and selectivity. Amongst the many carbon supports available, carbon nanofilaments (carbon nanotubes and carbon nanofibres) [3] and carbon xerogels [4-6] fulfill the mentioned requirements.

Carbon nanofilaments suffer, however, from technical drawbacks related with their powdery nature, which makes handling in catalytic processes troublesome. In particular, the use of powdery CNFs leads to agglomeration problems and difficulty of filtration in slurry phase operation, and pressure drop in gas phase operation. These inconveniences can be prevented by the incorporation of carbon filaments into larger objects like, for example, ceramic monoliths [7,8], sintered metal fibres or a carbon felt [9]. Another alternative could be the development of membranes consisting of entangled carbon nanofibers of a few tens of nanometer diameter obtained by electrospinning of a polymer followed by pyrolysis at high temperature [10,11].

The preparation of a ceramic monolith completely covered with a well-attached layer of carbon nanofibres (CNFs) of uniform thickness has been previously reported [7,8]. This method uses the catalytic decomposition of a hydrocarbon on a monolith coated with the growth catalyst. It was already shown that CNF/monoliths display relevant characteristics as catalyst support for several gas and liquid phase reactions. In gas phase reactions, the main advantage of using a CNF/monolith composite is its robustness, portability and low pressure drop. Besides, immobilization of CNFs avoids their release to the atmosphere with the associated risk for human health. Noble metal nanoparticles have been dispersed on monoliths coated with either CNFs or N-CNFs and used in NH_3 decomposition for in situ H_2 generation [12], for CO_2 conversion to hydrocarbons under high pressure conditions [13] or for catalytic combustion of BTX (benzene, toluene and xylene) at low temperatures (< 200 ºC) [14]. In the case of reactions carried out in liquid media, the main advantages of using a CNF/monolith compared to CNF slurries or bulky carbon pellets are that the filtration of the CNF slurry, which is a difficult step, can be avoided, and that diffusion of the reactants is faster due to the large mesopore volume and low tortuosity of CNFs, and to the short

diffusional path of the catalytic layer. For example, a CNF/monolith has been used as a Pd support for selective hydrogenation of cinnamaldehyde (CAL) [15], as a carrier for the immobilization of enzymes (lipase) in biocatalysis [16], as noble metal nanoparticle support for the reduction of nitrates and bromates in water [17,18] and as metal-free catalysts for the ozonation of organic pollutants in water [19].

In carbon xerogels, the size and volume of meso/macropores can be controlled by the synthesis procedures [20,21], including the synthesis variables (mainly the pH of the starting solution) and the drying and pyrolysis conditions of precursor gels. Regarding this last point, the evaporative drying technique was found to be the easiest and less expensive method for the synthesis of a porous carbon with a tailored texture, allowing all pore sizes to be obtained, but with the pore volume and the pore size strongly coupled. Carbon xerogels have been used to support both metal complexes [5,6,22] and metal nanoparticles [23], and the effect of the pore texture on mass transport was evidenced in gas phase and liquid phase catalysis [4,24], and in electrocatalysis [25].

As indicated above, both a CNF-monolith sample and a carbon xerogel with a proper mesoporous structure can be suitable catalyst supports to be used in gas or liquid phase reactions, in particular if the immobilized active phase is a relatively bulky molecular species. Consistently, the present work deals with the preparation of hybrid catalysts through the immobilization of an Rh diamine complex on the mentioned two carbon materials. The diamine Rh complex (schematically depicted in Figure 1) is $[Rh(COD)NH_2(CH_2)_2NH(CH_2)_3Si(OCH_3)_3]BF_4$, abbreviated as Rh(NN)Si. It contains a cyclooctadiene (COD) ligand and a bidentate amine ligand with a trimethoxysilane function ($-Si(OCH_3)_3$). As previously reported [26-28], the anchoring on the support is assumed to occur through a covalent siloxane-type bond created by reaction of methoxy functions with surface –OH type groups. It has been found that catalysts prepared in this way on different carbon materials are, in general, more active than the Rh(NN)Si in homogeneous phase and they are reusable [26-28]. Therefore, it was decided to extend the study to two structured carbon-based supports such as the CNF-monolith described above and a granular carbon xerogel. The main purpose of the study is to take advantage of both their open porous structure, which should decrease mass transfer limitations, and their morphology, which will facilitate the catalyst handling and will avoid difficult separation processes. Thus, compared to the previous studies, the present work is more

focused on the practical application of the catalysts and on a kinetic study of the process taking into account diffusional limitations.

2. Experimental

2.1. Supports

CNF coated monolith

The support was prepared by the following procedure [29]: a cordierite monolith (from Corning, 1 cm diameter, 5 cm length, 400 cpsi (channels per square inch)) was washcoated with alumina by dipcoating in a sol prepared with pseudoboehmite (AlOOH), urea and 0.3 M nitric acid with a weight ratio of 2:1:5. The liquid inside the monolith channels was removed by flushing pressurized air. Afterwards, the sample was dried at room temperature for 24 h while rotating around the longitudinal axis; it was then calcined in air at 873 K for 2 h. Nickel was deposited on the alumina washcoat as follows: the monolith sample was kept overnight in 1 L aqueous solution containing 29 g $Ni(NO_3)_2 \cdot 6H_2O$, 80 g NH_4NO_3 and 4 mL ammonia solution (25% w/w). This solution was flowing continuously through the channels. Then, the monolith was rinsed thoroughly with deionised water, dried (room temperature overnight, and 373 K for 1 h), and calcined in flowing nitrogen at 873 K for 2 h. The Ni content in the monolith was 0.9 wt%. After reduction (hydrogen atmosphere, 873 K, 2 h), the CNF were grown by putting the sample in contact with a 100 NmL/min flow of C_2H_6:H_2 mixture (molar ratio 1:1) at 873 K for 3.5 h. Development of CNFs follows a tip-growth model; indeed, the CNF diameter is similar to the diameter of the Ni nanoparticles on the Ni/Al_2O_3 monolith and encapsulated Ni nanoparticles are observed by TEM at the tip of some CNF [29].

The amount of CNF deposited corresponds to 15.5 wt% carbon and supposes an average layer thickness of about 10 µm. The BET surface area of CNF grown on the monolith is 150 m^2/g; they display a micropore volume of 0.01 cm^3/g and a mesopore volume equal to 0.30 cm^3/g [30]. The sample is named as M-CNF hereafter.

To prepare the catalyst, sample M-CNF was cut into several pieces of about 7 mm length that contained 20 to 30 mg of carbon. The cutting was done very carefully with a

metallic saw in order to avoid any fracture of the ceramic material. Figure 2 shows a picture of the original M-CNF sample and of several cut pieces.

Carbon xerogel

The carbon xerogel was prepared according to a reported procedure [21], which can be summarized as follows: the carbon gel was obtained by the polycondensation of resorcinol (R) and formaldehyde (F) in deionized water (R/F molar ratio = 0.5, dilution ratio D = 5.7), using a basic agent (Na_2CO_3, denoted C) to increase the pH of the solution. The R/C molar ratio was chosen equal to 750. Gelation was performed at 358 K for 72 h. Then, the sample was vacuum-dried at 333 K and heat treated (423 K, 12 Pa, 12 h) in order to obtain the organic xerogel. Finally, it was pyrolyzed under nitrogen flow (1073 K, 3 h), allowing the carbon xerogel material to be obtained. Prior to its use, the sample was grinded and sieved to ensure a particle size between 1.0 and 1.4 mm (Figure 3). The sample is named CX3.

Oxidation treatment

In order to develop surface oxygen complexes on both carbon supports, which is necessary to graft the Rh complex, the catalyst supports were submitted to an oxidation treatment under the following conditions: heating up to 623 K (15 K/min) was performed in He, then the gas flow was switched to synthetic air (60 NmL/min) with a soaking time of 3.5 h. Afterwards, the samples were cooled down in air and stored until use. The oxidized samples are named M-CNFOx and CX3Ox, respectively.

Characterization

The surface chemistry of the oxidized supports was characterized by TPD (temperature programmed desorption) using a thermobalance SDT TA Instruments 2960 coupled to a mass spectrometer Balzers MSC 200 Thermostar. Approximately 10 mg of carbon material (obtained by scrapping in the case of the M-CNF sample) were heated at 20 K/min up to 1300 K in a He flow of 20 NmL/min.

The textural properties of the supports were analyzed by N_2 adsorption at 77 K, using a Micromeritics ASAP 2020 device in the case of sample M-CNFOx and an automatic volumetric apparatus Autosorb-6B (Quantachrome) in the case of support CX3Ox. The

samples were previously outgassed at 523 K for 4 h. BET surface area (S_{BET}) and pore volumes of different size range (micropores, V_μ, and mesopores, V_{meso}) were determined as described in the literature [31]. It was checked by mercury porosimetry that the carbon materials do not contain macropores. The skeletal density (ρ_s) of the carbon structures, i.e. all open pores excluded, was measured by helium pycnometry using a Micromeritics Accupyc 1330 device. The bulk density was calculated from the previous data as:

$$\rho_{bulk} = \frac{1}{V_v + \frac{1}{\rho_s}} \quad (1)$$

where V_V is the total pore volume, i.e. the sum of mesopore and micropore volumes, V_{meso} and V_μ. The void fraction corresponding to mesopores in the carbon material can be calculated as:

$$\varepsilon = \frac{V_{meso}}{V_{meso} + V_\mu + \frac{1}{\rho_s}} \quad (2)$$

The supports were also characterized by transmission and scanning electron microscopy (TEM and SEM) using the JEOL JEM-2010 and HITACHI S-3000N microscopes, respectively.

2.2. Catalysts

The synthesis of the complex $[Rh(COD)NH_2(CH_2)_2NH(CH_2)_3Si(OCH_3)_3]BF_4$, (Rh(NN)Si) was carried out using standard Schlenk techniques and following the reported procedure [27]. The synthesized Rh complex was characterized by infrared spectroscopy (FT-IR), X-ray photoelectron spectroscopy (XPS) and elemental analysis (EA); the obtained results, which were reported elsewhere [26], indicated that the desired complex was obtained.

The hybrid catalysts were prepared by impregnation of the supports (previously outgassed at 373 K, 3 h) with a methanol solution of the Rh(NN)Si complex (5 mL solution per gram of support). The mixture was maintained under reflux for 21 h; then, the solid was removed from the solution and washed with methanol in Soxhlet for 24 h. Afterwards, the catalysts were vacuum-dried (0.01 Pa) at room temperature for 24 h.

The hybrid catalysts are named as M-CNFOx-Rh and CX3Ox-Rh. The actual amount of loaded Rh, was 0.4 wt% (39 μmol/g) in both samples, as determined by ICP-OES using the methodology described in the literature [27]. In the case of support M-CNFOx, this percentage was calculated with respect to the mass of CNF deposited on the ceramic monolith.

The catalysts were characterized by XPS in a VG Microtech Multilab 3000 spectrometer, and by TEM (both, fresh and used catalyst) using the same equipment as in the case of the supports.

2.3. Catalytic activity

Catalytic activity for the hydrogenation of cyclohexene was measured. Reactions were carried out in a stainless steel Parr reactor (40 mL, diameter = 2 cm), magnetically stirred, and equipped with a gas inlet valve for charging and purging the gas into the reactor and a pressure gauge for the pressure control. The experimental setup also allows monitoring the hydrogen consumption during the reaction.

The M-CNFOx-Rh catalyst sample used was a 7 mm long piece, with about 20 mg CNF, while about 20 mg of catalyst CX3Ox-Rh were used. The M-CNFOx-Rh catalyst piece was suspended into the reactor by means of a yarn (Figure S1) and fixed on the reactor top. In a typical experiment, the mentioned amount of catalyst and 10 mL of a 5 vol% cyclohexene in methanol solution were used. The reactor was pressurized with He and purged three times; the reactor was then filled with H_2 and evacuated three times to finally set the H_2 pressure to 1 MPa. Afterwards, the reactor was placed in the thermostatic bath at 333 K and the stirring (1100 rpm) was started. An homogeneous phase reaction was also carried out with the Rh(NN)Si complex in solution, using the proper amount of the complex dissolved in methanol and keeping all the mentioned conditions.

Previously, blank experiments without catalyst and with the support yielded cyclohexene conversion after 20 h of 8% and 5%, respectively. These tests indicated that, in the absence of the Rh complex, the extent of the reaction is negligible compared to that of the catalyzed systems.

Reactants and products were analyzed by gas chromatography using the HP 6890 equipment with a FID detector and a HP-1 Methyl Siloxane column (30 m-250 mm-0.25 mm).

3. Results and discussion

3.1. Characterization of supports and catalysts

Relevant data on the textural properties of the carbon materials used as support are collected in Table 1, which includes BET surface area (S_{BET}), micropore volume (V_μ), mesopore volume (V_{meso}), bulk density (ρ_{bulk}), skeletal density (ρ_s) and void fraction (ε); all parameters are expressed per mass or volume unit of carbon. The average and maximum pore size of each material are also included in Table 1.

Table 1. Textural properties of the oxidized carbon materials used as supports.

Sample	S_{BET} (m^2/g)	V_μ (cm^3/g)	V_{meso} (cm^3/g)	ρ_{bulk} (g/cm^3)	ρ_s (g/cm^3)	ε (-)	$w_{p,av}$ (nm)	$w_{p,max}$ (nm)
M-CNFOx	150	0.01	0.30	1.3	2.0	0.38	23	80
CX3Ox	637	0.31	1.00	0.55	2.2	0.56	20	40

The two carbon materials display very different morphology and also very different textural properties. It is interesting to note the larger mesopore volume of the carbon xerogel. The layer of carbon nanofibers (CNF) has a negligible micropore volume (calculated by the t-plot method) and a significantly smaller specific surface area than the carbon xerogel support. The obtained values of surface area and pore volume are in agreement with those reported in the literature for CNF aggregates [32].

The TPD profiles of samples M-CNFOx (scrapped carbon nanofibres) and CX3Ox are shown in Figures 4a and 4b, respectively. The quantification of the TPD profiles of Figure 4 is shown in Table 2. Data corresponding to the non-oxidized samples (M-CNF and CX3) are also included to better appreciate the effect of the oxidation treatment. The amount of phenol type groups was determined by deconvolution of the CO evolution profile in the temperature range of 873-973 K [33-36] using the Origin software.

Table 2. Quantification of TPD profiles: amounts of evolved CO_2 and CO, total oxygen (weight percentage), and amount of phenol-type groups.

Sample	CO_2 (µmol/g)	CO (µmol/g)	O (wt. %)	Phenol-type groups [a] (µmol/g)
M-CNF	242	1868	3.8	520
M-CNFOx	457	1878	4.5	582
CX3	471	1101	3.3	314
CX3Ox	756	2021	5.7	858

[a] Determined by deconvolution of the CO desorption profile.

CO_2 evolution from sample M-CNFOx shows a maximum at about 770 K. This peak can be assigned to the decomposition of lactone and anhydride-type surface oxygen groups. The CO evolution starts at about 670 K and the profile suggests the presence of several CO-type groups of different thermal stability, like anhydride, phenol, carbonyl and quinone [33-36]. The oxidation treatment with air leads to an increase of the surface oxygen complexes that decompose as CO_2, while the amount of CO-type groups remains almost unchanged.

The CO_2 evolution profile of sample CX3Ox is wider (CO_2 desorption occurs from 700 to 1100 K), suggesting the presence of oxygen surface groups like anhydride and lactone. The CO evolution starts at a relatively high temperature and shows a maximum around 1000 K, showing the presence of a high amount of phenol and carbonyl-type groups on the sample surface. Both CO_2- and CO-type groups were generated by oxidation of the CX3Ox sample with air. The TPD data show that the oxidation treatment is more effective in the carbon xerogel than in the grown CNF. Notwithstanding, both samples contain enough phenol-type groups to ensure the anchoring of the complex (three mol of phenol-type groups per mol of Rh complex, see Figure 1).

Morphological and structural information of the supports was obtained by TEM analysis. Figure 5a shows TEM images of the carbon nanofibres of sample M-CNFOx. The CNFs display a fishbone structure, with diameter ranging from 10 to 20 nm. Figure

5b shows the TEM image of sample CX3Ox that presents a spongy appearance and a tortuous pore network.

The parameters determined from the XPS analysis of catalysts M-CNFOx-Rh and CX3Ox-Rh are presented in Table 3. These data show that the electronic state of Rh is almost unmodified upon heterogenization and corresponds to Rh(I). The binding energy found for N1s is characteristic of N in amine and is similar to that measured for the homogeneous complex [37]. The factor F, calculated as the ratio between the amount of Rh determined by XPS and by ICP ($F = Rh_{XPS}/Rh_{ICP}$), is close to 4 for both catalysts. This indicates that the spatial distribution of the complex along the support depth is similar in both catalysts. This result is similar to that previously found with catalysts prepared with carbon nanotubes and nanofibres, where F values close to 4 were reported [27], and lower than those reported for catalysts prepared with a microporous activated carbon (F values between 10 and 20) [38]. Thus, it can be considered that the Rh complex molecules are likely more internally located in the present case than in microporous activated carbon.

Table 3. XPS data of the Rh(NN)Si complex and the hybrid catalysts.

Sample	Binding energy (eV)		$F=Rh_{XPS}/Rh_{ICP}$
	$Rh3d_{5/2}$	N1s	
Rh(NN)Si	309.1	400.3	-
M-CNFOx-Rh	309.0	401.0	4
CX3Ox-Rh	308.7	400.5	4

3.2.Catalytic activity

Figure 6 shows the cyclohexene conversion versus time profiles obtained for the hybrid catalysts and the homogeneous Rh(NN)Si complex. These conversion data were determined from hydrogen consumption versus time curves. TOF (s^{-1}) values determined at 40 min reaction time and using the initial Rh loading, are also shown in Figure 6 (see inset).

Data of Figure 6 show that the hybrid catalysts lead to a noticeably higher conversion than the unsupported Rh complex. This was also observed for other carbon-based hybrid catalysts and it was explained by the potential confinement of the active species in the support porosity [26,27,39]. From about 1 h on, both heterogeneous catalysts display similar conversion values, even though M-CNFOx-Rh gives a higher conversion in the first 30 min. One however notices that the conversion profile of CX3Ox seems more linear than that of M-CNFOx. The reasons for this change of apparent reaction rates are not clear at the moment but could be due either to external/internal mass transport effects or to a modification of the reaction pathway.

The conversion profiles of both hybrid catalysts reveal different kinetics. In the case of sample CX3Ox-Rh, the linear variation of conversion with time in the first 40 minutes suggests a 0 reaction order, maybe due to diffusional problems. Such a phenomenon has been recently reported in liquid-phase reactions performed using carbon xerogels supported catalyst [24]. The different morphology of the two hybrid catalysts bears differences in the diffusional path length. As indicated above, the CNF coating has an average thickness of 10 µm while for the 1-1.4 mm particles of CX3Ox-Rh the diffusional path is about 500-700 µm, meaning that diffusional limitations are very likely to occur in this latter catalyst.

Thus, although the hybrid catalysts are clearly more active than the homogeneous complex, their apparent activity could be lower than their intrinsic activity due to diffusional limitations, particularly in the case of the CX3Ox-Rh catalyst. It was attempted to check for the existence of internal diffusional limitations via the estimation of the Weisz modulus, as described in reference [24]. The Weisz modulus (Φ) is defined as the ratio between the apparent specific reaction rate and the diffusion rate of reactants in the catalyst particle. For Φ larger than 1, the internal diffusion limitations become rate-determining. The Weisz modulus is calculated by equation (2) [40], at the beginning of the reaction:

$$\Phi = \frac{r_s L_p^2}{D_e \; C_s} \qquad (2)$$

where r_s is the initial apparent specific reaction rate per unit of catalyst volume (kmol m_{cat}^{-3} s^{-1}), L_p is the characteristic dimension of the catalytic media (i.e. 1/6th of the particle diameter for spherical catalyst pellets or thickness in the case of a flat active layer accessible from one side), C_s is the reactant concentration at the external particle surface, and D_e is the effective diffusivity through the catalyst pores. Fast stirring of the reactor allows to assimilate it to a perfectly mixed tank so that the reactant concentration at the external particle surface C_s is assumed to be close to the reactant concentration in the solution bulk at the beginning of the reaction ($C_e = 0.49\times10^3$ mol/m^3, corresponding to 5% vol. cyclohexane in methanol). The effective diffusivity is defined by:

$$D_e = \frac{\varepsilon\ D_m}{\tau} \sim \varepsilon^2 D_m \tag{3}$$

where D_m is the molecular diffusivity of the considered component (~10^{-9} m²/s for diffusion in liquids), ε is the void fraction of the catalyst and τ is tortuosity of the catalyst pores. The initial apparent specific reaction rate, r_s, is calculated from the slope of the conversion vs. time curve:

$$r_s = C_e \left(\frac{dX}{dt}\right)_{t=0} V_R \frac{\rho_{bulk}}{m_{catal}} \tag{1}$$

where $\left(\frac{dX}{dt}\right)_{t=0}$ is the slope at zero time of the tangent of the conversion curves (s^{-1}) (Figure 6), V_R is the reactor volume (10×10^{-6} m^3 of reacting fluid), ρ_{bulk} is the bulk density of the catalyst (kg/m^3) which depends on the catalyst support (Table 1), and m_{catal} is the mass of catalyst used for each experiment (20×10^{-6} kg).Globally, the differences between the two systems are: (i) the void fraction of the support (0.38 vs. 0.56 for M-CNFOx and CX3Ox, respectively), (ii) the characteristic length of the catalyst (10×10^{-6} m for M-CNFOx; 10^{-3}/6 m for CX3Ox, assuming spherical particles), and (iii) r_s (estimated, from Figure 6, equal to about 451 and 76 kmol m_{cat}^{-3} s^{-1} for M-CNFOx-Rh and CX3Ox-Rh, respectively). From the data gathered, Φ was found to be equal to 0.6 in the case of the M-CNFOx supported catalyst and to 13 for the carbon xerogel-supported catalyst. In the latter case, mass transport limitations are clearly present, leading to a decrease of the catalytic activity with regard to chemical regime. In the former case, mass-transport limitations cannot be totally excluded since Φ is not much lower than 1 (please keep in mind that many values used are estimations), but

these limitations are certainly less severe than in the case of the carbon xerogel. These calculations highlight the fact that, especially in liquid phase, an open texture such as that encountered in carbon xerogels does not guarantee the absence of internal limitations. It is worth noticing that the pore size has no effect. In fact, the modification of the Weisz modulus between the two catalysts is mainly due to the difference in characteristic lengths, L_p.

In order to decrease mass transport effects in the case of CX3Ox-Rh, one could envisage grinding the catalyst particles, which would lead to a decrease of L_p. However, smaller particles would be more difficult to filter and recover. So, from a technical point of view, a potential higher effectiveness is sacrificed for a better handling when particles around 1 mm are used. Note also that, despite strong stirring, the absence of external mass transport limitations is not guaranteed, especially in the case of the xerogel-supported catalyst. Indeed, since the particles are mobile, one can consider that they are more or less immobile with the adjacent fluid, which could lead to non-negligible diffusion layer thickness. The existence of external diffusional limitations is however, in this case difficult to check; a deeper investigation, which is out of the scope of the present study, would be necessary to conclude with certainty. Finally, one could also try to combine the high void fraction and specific surface area of carbon gels with the advantages of small L_p by depositing a layer of carbon gel at the surface of the monolith used for CNT growth. This would allow decreasing the mass transport effects encountered in carbon gels while keeping easy handling. Such a support has not been prepared yet and could be interesting for further studies, even though the carbon adhesion to the support might be difficult to guarantee, especially since the RF organic gel shrinks upon pyrolysis. This could however be a good way to combine the advantages of both materials.

After the first catalytic run (t = 1.5 h), and in order to study its reusability, the hybrid catalyst was removed from the reaction media, washed with fresh solvent and used again in a catalytic run under the same conditions. Catalyst CX3Ox-Rh was removed by filtration while catalyst M-CNFOx-Rh, due to its morphology, could be much easily withdrawn from the reaction media (Figure S1).

Figure 7 shows the cyclohexene conversion profiles corresponding to the first and second catalytic runs, together with the corresponding TOF at 50% conversion; TOF was calculated with the initial Rh loading. Data in Figure 7 show that both catalysts are fully recyclable; even better, the catalytic activity increased significantly in the second run compared to the first one. Nevertheless, the difference in activity between the two catalysts is kept in the second run.

Determination of the amount of Rh in the used catalysts shows that leaching in both catalysts is not an issue (below 4%). The used catalysts were also analyzed by XPS and the obtained results can be summarized as follows: (i) in catalyst CX3Ox-Rh, Rh is present as Rh(I) (BE (Rh $3d_{5/2}$) = 309.9 eV) (60%) and Rh(0) (BE (Rh $3d_{5/2}$) = 307.8 eV) (40%) and no significant change of the F factor; (ii) in catalyst M-CNFOx-Rh, the Rh signals were too weak for a proper analysis; (iii) in both cases the BE of N1s is 400.9 eV, unveiling the presence of amines. These data indicate that a partial reduction of the metal complex takes place in catalyst CX3Ox-Rh, which is also expected in the case of M-CNFOx-Rh. It also indicates that, in the latter case, Rh species have likely migrated to a more inner location, becoming thus less accessible to the X-ray radiation.

TEM analysis of the used catalysts shows the presence of small metal particles in both of them (Figure 8), in agreement with the partial reduction of the supported metal complex under reaction conditions observed by XPS. Size measurement of more than one hundred particles led to data shown in Figure 9.

These data show that the development of metal particles is different on both supports, being clearly smaller in catalyst M-CNFOx-Rh. This fact can be the consequence of a different interaction of the Rh complex with the two supports in agreement with previous results showing that the support has a strong influence on the properties of the hybrid catalyst [26]. The mentioned article demonstrated that the surface of carbon xerogels contributes to the stabilization of the small metallic particles, whereas significant sintering takes place on massive carbon nanofibers. In the present case, the smallest particles are developed on the carbon nanofibers, which are not massive but with a fishbone structure. However, it is not possible to confirm any difference regarding the degree of reduction of the metal complex in both catalysts. According to

the XPS data commented above, the active species in catalyst CX3Ox is a mixture of the supported complex Rh(NN)Si and small metallic Rh particles. In the case of catalyst M-CNFOx-Rh something similar can be assumed although it was not technically possible to be determined by XPS.

The development of small metal particles could explain the increase of the catalytic activity in the second run, although, as previously suggested, some modifications of the metal complex can also lead to more active species. The most reliable proposed modification is a change in the metal coordination sphere by hydrogenation of the cyclooctadiene ligand [38].

The obtained results show that catalysts M-CNFOx-Rh and CX3Ox-Rh are noticeably more active than the homogeneous Rh complex, stable against leaching and reusable. They are, as well, more active than similar catalysts prepared previously using other carbon xerogels of different porous texture or massive carbon nanofibres [26]. Moreover, catalyst M-CNFOx-Rh shows further advantages like the easy handling, the immediate recovery and removal from the reaction media avoiding the need of a filtration step, good mechanical strength, and the potential to fix the catalyst to operate in continuous mode with low pressure drop.

4. Conclusions

Hybrid catalysts were prepared by anchoring covalently an Rh diamine complex on two very different structured carbon materials: a ceramic monolith coated with carbon nanofibres and a mesoporous carbon xerogel. The morphology of these catalysts allows an easy separation from the reaction media. The obtained catalysts are noticeably more active than the homogeneous Rh complex and are stable against leaching. After a first use, a partial reduction of the Rh complex takes place and nanometer-sized Rh particles are developed, which increases the catalyst activity. The catalyst prepared with the ceramic monolith coated with carbon nanofibres bear noteworthy advantages like easy handling, immediate recovery from the reaction media, and good mechanical strength.

Acknowledgement: The authors thank the financial support through public projects of reference: MAT2012-32832 (Spanish Ministry of Economy and Competitiveness and FEDER) and

PROMETEO/II/2014/010 (Generalitat Valenciana). CCG thanks her FPU scholarship to the Spanish Ministry of Education.

5. References

1. E. Auer, A. Freund, J. Pietsch, T. Tacke, Appl. Catal. A: Gen. 173, 2 (1998) 259-271.

2. P. Serp, J. L. Figueiredo, Carbon Materials for Catalysis, John Wiley & Sons, Inc., 2009.

3. P. Serp, M. Corrias, P. Kalck, Appl. Catal. A: Gen. 253, 2 (2003) 337-358.

4. N. Job, B. Heinrichs, S. Lambert, J.P. Pirard, J.F. Colomer, B. Vertruyen, J. Marien, AIChE J. 52, 8 (2006) 2663-2676.

5. N. Mager, N. Meyer, A.F. Léonard, N. Job, M. Devillers, S. Hermans, Appl. Catal. B: Environ. 148-149 (2014) 424-435.

6. B.F. Machado, H.T. Gomes, P. Serp, P. Kalck, J.L. Figueiredo, J.L. Faria, Catal. Today 149, 3-4 (2010) 358-364.

7. E. García-Bordejé, I. Kvande, D. Chen, M. Ronning, Adv. Mater. 18, 12 (2006) 1589-1592.

8. N.A. Jarrah, J.G. van Ommen, L. Lefferts, J. Mater. Chem. 14, 10 (2004) 1590-1597.

9. P. Yaseneva, C.F. Marti, E. Palomares, X. Fan, T. Morgan, P.S. Perez, M. Ronning, F. Huang, T. Yuranova, L. Kiwi-Minsker, S. Derrouiche, A.A. Lapkin, Chem. Eng. J. 248 (2014) 230-241.

10. C. Kim, B.T.N. Ngoc, K.S. Yang, M. Kojima, Y.A. Kim, Y.J. Kim, M. Endo, S.C. Yang, Adv. Mater. 19, 17 (2007) 2341-2346.

11. Y. Qiu, J. Yu, T. Shi, X. Zhou, X. Bai, J.Y. Huang, J. Power Sources 196, 23 (2011) 9862-9867.

12. S. Armenise, L. Roldán, Y. Marco, A. Monzón, E. García-Bordejé, J. Phys. Chem. C 116, 50 (2012) 26385-26395.

13. D.R. Minett, J.P. O'Byrne, S.I. Pascu, P.K. Plucinski, R.E. Owen, M.D. Jones, D. Mattia, Catal. Sci. Technol. 4, 9 (2014) 3351-3358.

14. S. Morales-Torres, A.F. Pérez-Cadenas, F. Kapteijn, F. Carrasco-Marín, F.J. Maldonado-Hódar, J.A. Moulijn, Appl. Catal. B: Environ. 89, 3-4 (2009) 411-419.

15. J. Zhu, Y. Jia, M. Li, M. Lu, J. Zhu, Ind. Eng. Chem. Res. 52, 3 (2013) 1224-1233.

16. K.M. De Lathouder, J.J.W. Bakker, M.T. Kreutzer, S.A. Wallin, F. Kapteijn, J.A. Moulijn, Chem. Eng. Res. Des. 84, 5 (2006) 390-398.

17. Y. Marco, E. García-Bordejé, C. Franch, A.E. Palomares, T. Yuranova, L. Kiwi-Minsker, Chem. Eng. J. 230 (2013) 605-611.

18. T. Yuranova, L. Kiwi-Minsker, C. Franch, A.E. Palomares, S. Armenise, E. García-Bordejé, Ind. Eng. Chem. Res. 52, 39 (2013) 13930-13937.

19. J. Restivo, J.J.M. Órfão, M.F.R. Pereira, E. García-Bordejé, P. Roche, D. Bourdin, B. Houssais, M. Coste, S. Derrouiche, Chem. Eng. J. 230 (2013) 115-123.

20. N. Job, R. Pirard, J. Marien, J.P. Pirard, Carbon 42, 3 (2004) 619-628.

21. N. Job, A. Théry, R. Pirard, J. Marien, L. Kocon, J.N. Rouzaud, F. Béguin, J.P. Pirard, Carbon 43, 12 (2005) 2481-2494.

22. F. Maia, N. Mahata, B. Jarrais, A.R. Silva, M.F. Pereira, C. Freire, J.L. Figueiredo, J. Mol. Catal. A: Chem. 305, 1-2 (2009) 135-141.

23. E. Bailón-García, F. Carrasco-Marín, A.F. Pérez-Cadenas, F.J. Maldonado-Hódar, Catal. Comm. 58 (2015) 64-69.

24. S.L. Pirard, C. Diverchy, S. Hermans, M. Devillers, J.P. Pirard, N. Job, Catal. Comm. 12, 6 (2011) 441-445.

25. N. Job, J. Marie, S. Lambert, S. Berthon-Fabry, P. Achard, Energy Convers. Manag. 49, 9 (2008) 2461-2470.

26. C.C. Gheorghiu, C. Salinas Martínez de Lecea, M.C. Román Martínez, ChemCatChem 5, 6 (2013) 1587-1597.

27. L.J. Lemus-Yegres, M.C. Román-Martínez, I. Such-Basáñez, C. Salinas-Martínez de Lecea, Microporous Mesoporous Mater. 109, 1-3 (2008) 305-316.

28. L.J. Lemus-Yegres, M. Pérez-Cadenas, M.C. Román-Martínez, C. Salinas-Martínez de Lecea, Microporous Mesoporous Mater. 139, 1–3 (2011) 164-172.

29. E. García-Bordejé, I. Kvande, D. Chen, M. Rønning, Carbon 45, 9 (2007) 1828-1838.

30. S. Armenise, M. Nebra, E. García-Bordejé, A. Monzón, in: Gaigneaux, E.M. (Ed.), Studies in Surface Science and Catalysis Scientific Bases for the Preparation of Heterogeneous Catalysts - Proceedings of the 10th International Symposium, Louvain-la-Neuve, Elsevier,2010, pp. 483-486.

31. F. Rodríguez-Reinoso, A. Linares-Solano, Chemsitry and Physics of Carbon, New York: Dekker, 1988.

32. K.P. de Jong, J.W. Geus, Catal. Rev. 42, 4 (2000) 481-510.

33. J.L. Figueiredo, M.F.R. Pereira, M.M.A. Freitas, J.J.M. Órfão, Carbon 37, 9 (1999) 1379-1389.

34. S. Haydar, C. Moreno-Castilla, M.A. Ferro-García, F. Carrasco-Marín, J. Rivera-Utrilla, A. Perrard, J.P. Joly, Carbon 38, 9 (2000) 1297-1308.

35. G.S. Szymanski, Z. Karpinski, S. Biniak, A. Swiatkowski, Carbon 40, 14 (2002) 2627-2639.

36. J.H. Zhou, Z.J. Sui, J. Zhu, P. Li, D. Chen, Y.C. Dai, W.K. Yuan, Carbon 45, 4 (2007) 785-796.

37. http://www.lasurface.com/accueil/index.php

38. L.J. Lemus-Yegres, I. Such-Basáñez, M.C. Román-Martínez, C. Salinas-Martínez de Lecea, Appl. Catal. A: Gen. 331 (2007) 26-33.

39. S. Pariente, P. Trens, F. Fajula, F. Di Renzo, N. Tanchoux, Appl. Catal. A: Gen. 307, 1 (2006) 51-57.

40. G.F. Froment, K.B. Bischoff, J. de Wilde, Chemical Reactor Analysis and Design, 3rd Edition, John Wiley and Sons, 2011.

Figure captions

Figure 1. Chemical structure of the Rh(NN)Si complex.

Figure 2. Pictures of the CNF-coated monolith sample (M-CNF): original form and cut pieces.

Figure 3. Pictures of the carbon xerogel CX3 sample: (a) original form and (b) grinded (1.0-1.4 mm).

Figure 4. TPD profiles of: (a) M-CNFOx and (b) CX3Ox.

Figure 5.TEM images of (a) fibres of M-CNFOx sample and (b) CX3Ox.

Figure 6. Cyclohexene conversion versus time of the homogeneous Rh(NN)Si complex and hybrid catalysts and TOF (at 40 min, calculated with the initial Rh loading) (5 vol% cyclohexene in methanol, 10 bar H_2, 333 K, 1100 rpm).

Figure 7. Cyclohexene conversion versus time and TOF (at 50% conversion, calculated with the initial Rh loading), in two consecutive catalytic runs (5 vol% cyclohexene in methanol, 10 bar H_2, 333 K, 1100 rpm).

Figure 8. TEM images of used catalysts: (a) and (b) CX3Ox-Rh and (c) and (d) M-CNFOx-Rh.

Figure 9. Particle size distribution based on a particle count of at least 100 elements.

Figure S1. Location in the reactor and removal from it, of catalyst M-CNFOx-Rh.

Figure 1

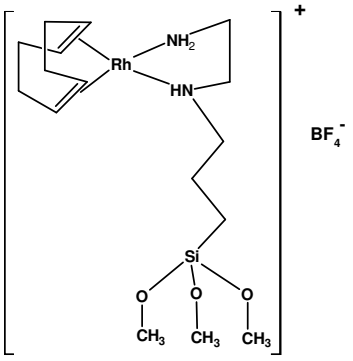

Figure 2

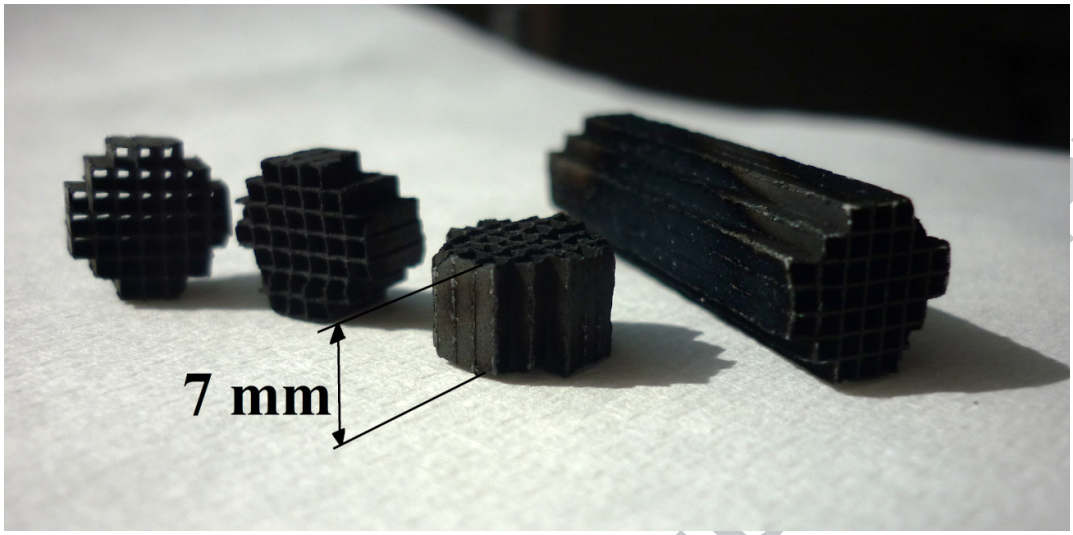

Figure 3

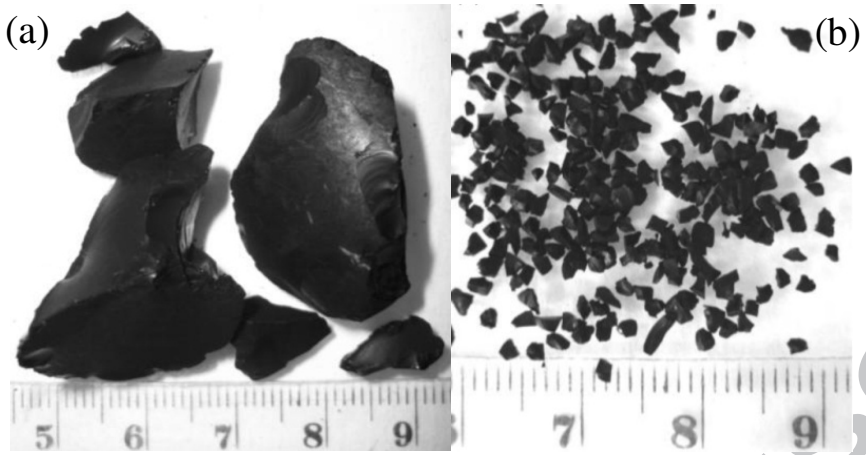

Figure 4

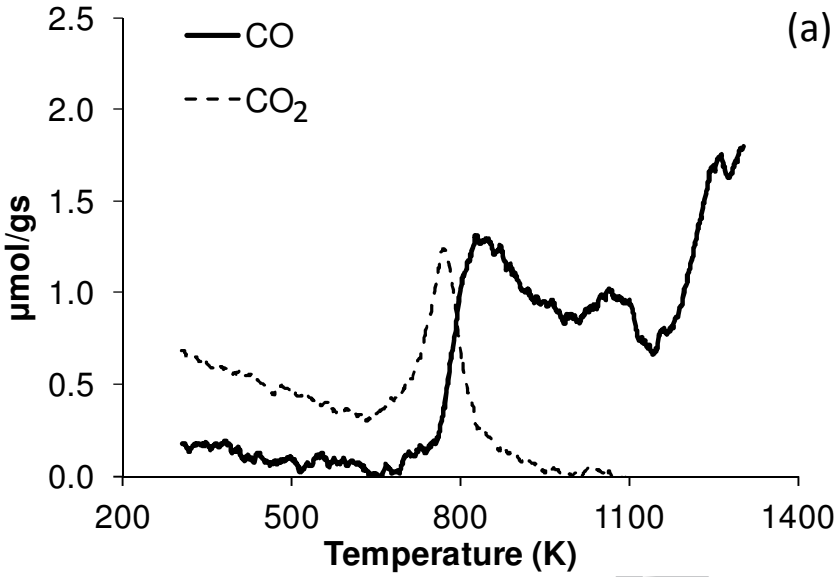

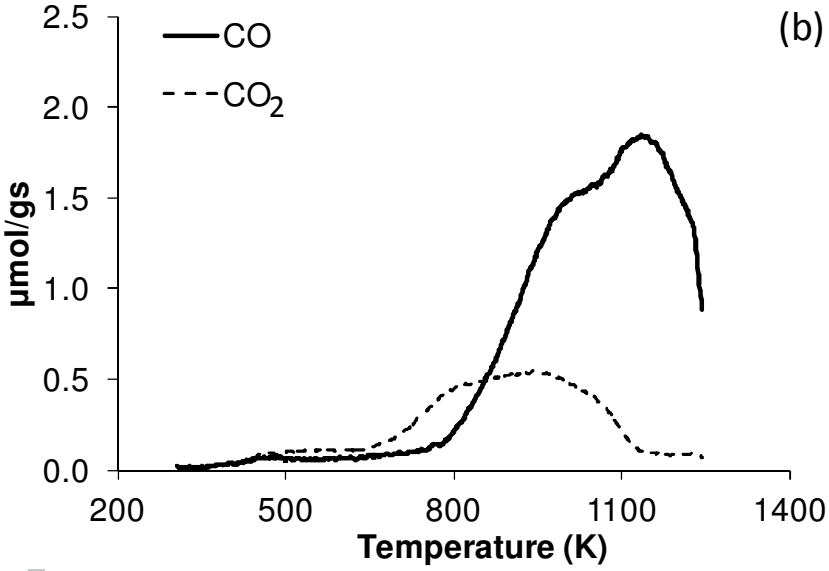

Figure 5

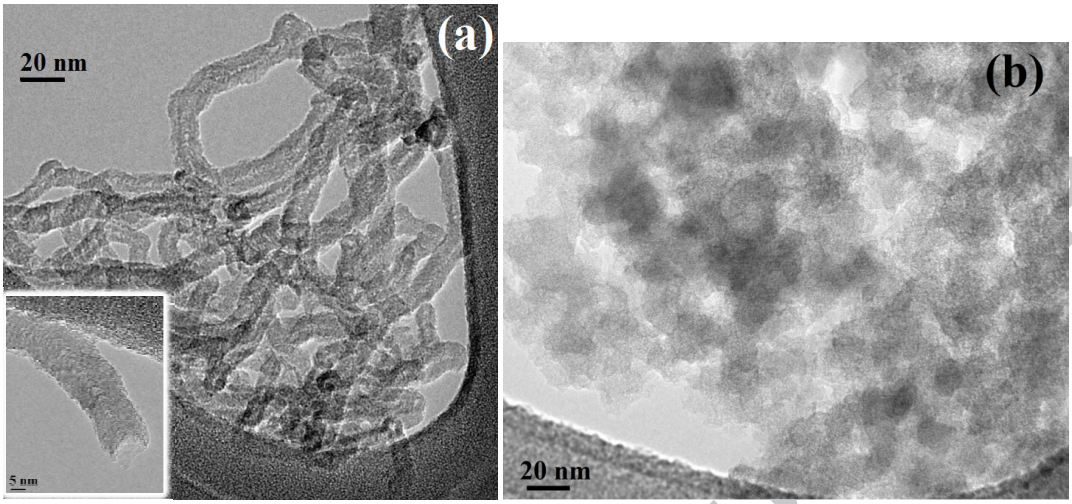

Figure 6

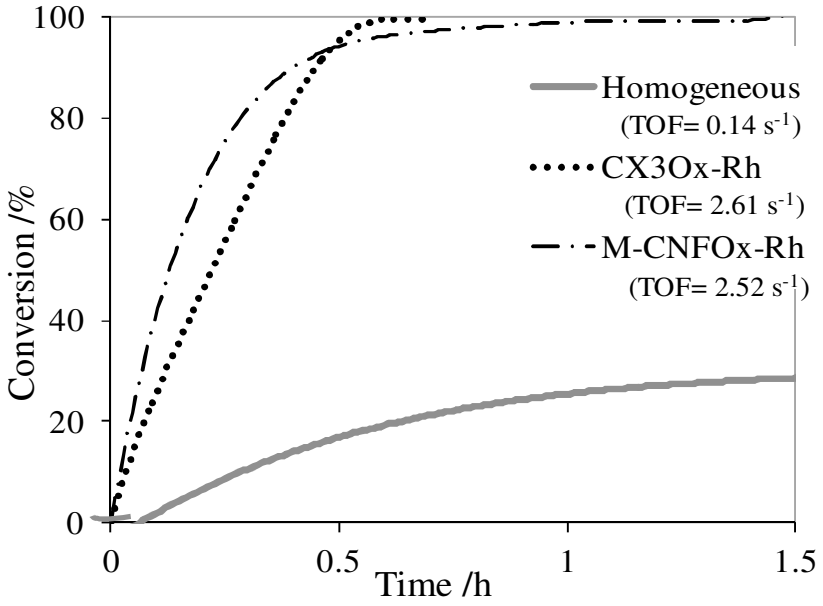

Figure 7

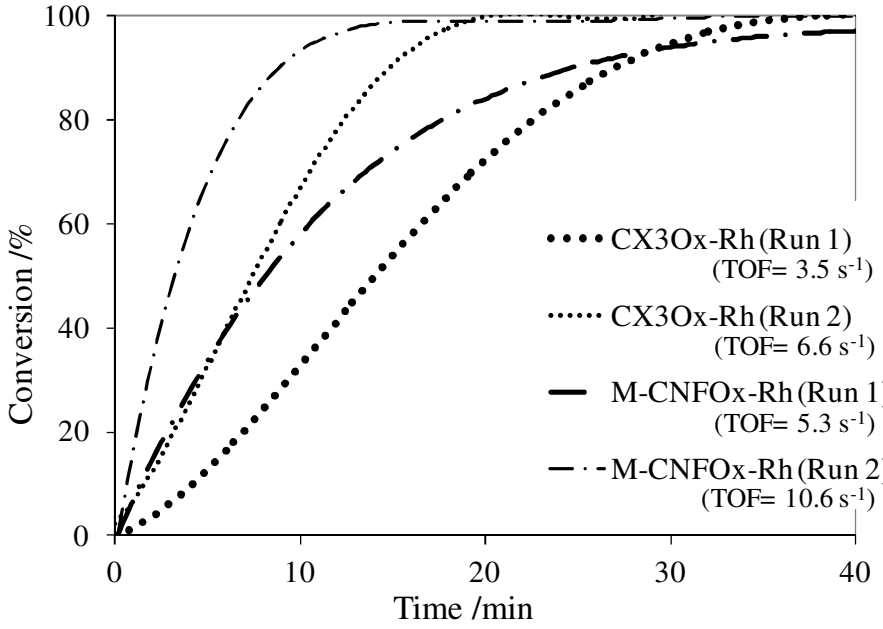

Figure 8

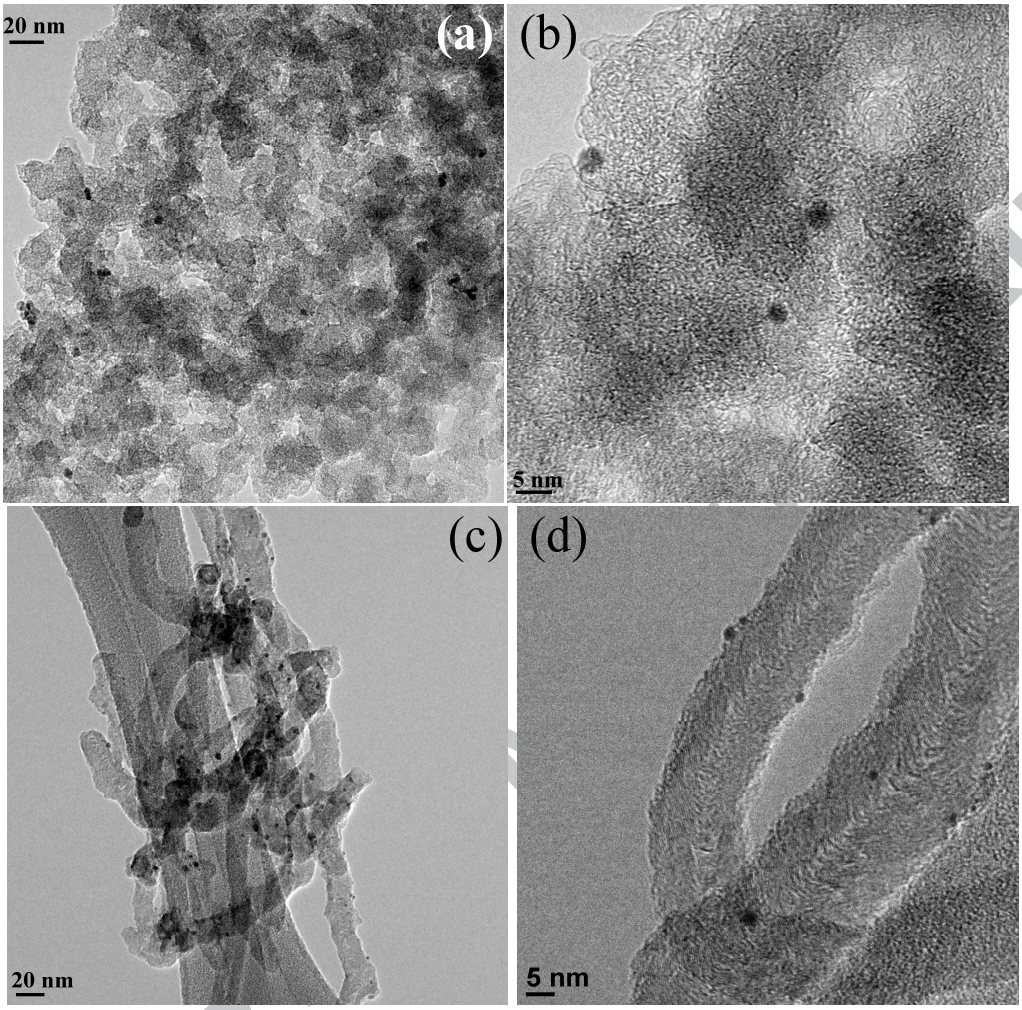

Figure 9

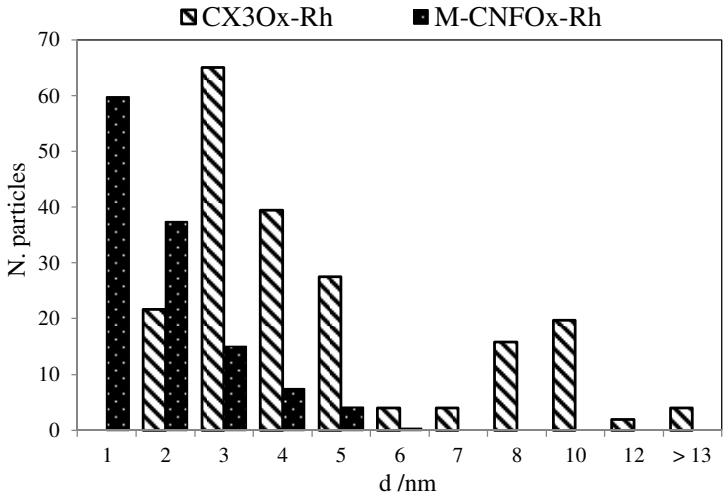

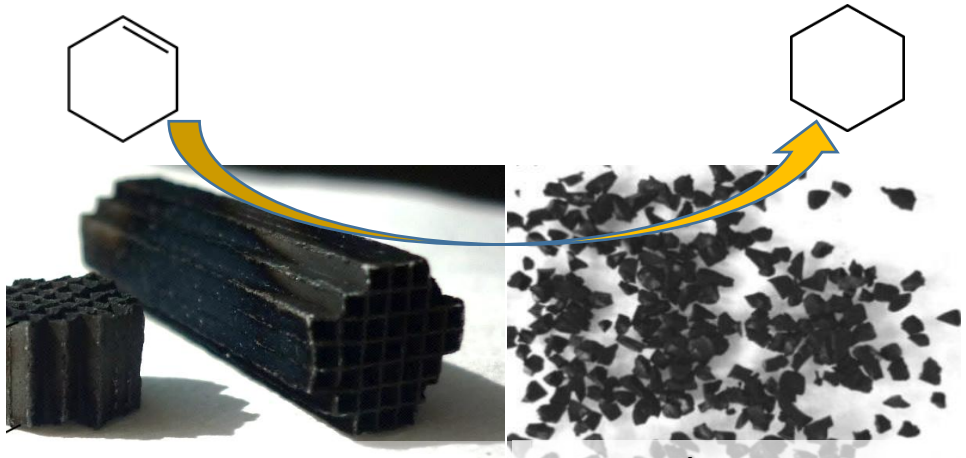

Rh complex/CNF-monlith

Rhcomplex/carbon xerogel

Easy handling

Research highlights

- CNF-monolith and granular carbon xerogel are used as supports in hybrid catalysts
- The supports have open porous structure, and a morphology that facilitates handling
- The catalysts are more active than the homogeneous Rh complex and are leaching-stable
- Despite the open porous structure, mass transport limitations are present